First International Symposium on Marine Propulsors
smp'09, Trondheim, Norway, June 2009

Unsteady Analysis of a Horizontal Axis Marine Current Turbine in Yawed Inflow Conditions With a Panel Method

J. Baltazar, J.A.C. Falcão de Campos

Marine Environment and Technology Center (MARETEC),
Department of Mechanical Engineering, Instituto Superior Técnico (IST), Lisbon, Portugal

ABSTRACT

A low order potential based panel method is used for the analysis of the unsteady flow around marine current turbines. An empirical vortex model independent of the induced velocities is assumed for the turbine wake. The analysis is carried out for a controllable pitch horizontal axis marine current turbine in straight and yawed inflow conditions at two different pitch settings in a wide range of tip-speed-ratios. The results are compared with experimental data from the literature and with the lifting line theory. A fair to good agreement with the experimental performance data is found near the design condition. The effect of the viscous corrections on the prediction of turbine performance coefficients is illustrated.

Keywords

Marine Current Turbine, Panel Method, Performance Predictions.

1 INTRODUCTION

There has been a growing interest in the utilisation of marine current turbines for electrical power production. The ability to predict the hydrodynamic performance of a marine current turbine is essential for the design and analysis of such systems.

Marine current turbines operate in a non-uniform inflow due to variations on the tidal direction and to the site velocity profile. Due to these spatial variations on the inflow, the turbines blades are subject to time-dependent inflow conditions causing an unsteady flow field around the blades. This flow field is responsible for unsteady loads on the blades which are important for the analysis of fatigue loadings, and, possibly, for the occurrence of unsteady cavitation phenomena.

The analysis of the potential flow around marine current turbines may be carried out with a Boundary Element Method, also known as Panel Method. This method is likely to provide useful information on the pressure distributions around blades and form the basis for predicting blade cavitation performance. This method has been widely used in the hydrodynamic analysis of marine propellers, see, for instance Kerwin et al. (1987).

This paper presents the application of a panel code (PROPAN) to the analysis of marine current turbines. The code has been under development at MARETEC/IST for the hydrodynamic analysis of marine propulsors, (Baltazar, 2008) and (Baltazar and Falcão de Campos, 2006).

The analysis is carried out for axial and yawed inflow conditions for a turbine with controllable pitch for two different pitch settings in a wide range of tip-speed-ratios. An empirical vortex model independent of the induced velocities is assumed for the turbine wake. Comparison of numerical results with experimental measurements available in the literature, (Bahaj et al., 2007b), and the influence of viscous effects on the turbine blade forces are presented.

2 MATHEMATICAL FORMULATION

2.1 Potential Flow Problem

Consider the rotor of a horizontal axis turbine with radius R placed in a fluid stream and rotating at constant angular velocity Ω around its axis. The turbine rotor is made of K blades symmetrically distributed around a hub. We introduce a Cartesian coordinate system (x_0, y_0, z_0) fixed with the turbine and a Cartesian coordinate system (x, y, z) rotating with the turbine rotor. Figure 1 shows the turbine rotor and the two coordinate systems used to describe the flow field.

The x and x_0 axes of the two coordinate systems coincide with the turbine rotation axis and are reckoned positive pointing in the downstream flow direction. The y_0 and z_0 are at the turbine plane, with y_0 pointing upwards and z_0 completing the right-hand system. The y axis is coincident with the turbine reference line, passing through the reference point at the root section of the $k = 1$ blade (or key blade) and z completes the right-hand system. We introduce cylindrical coordinate systems (x_0, r_0, θ_0) and (x, r, θ) related to the Cartesian systems by

$$y_0 = r_0 \cos\theta_0, \quad z_0 = r_0 \sin\theta_0, \quad y = r\cos\theta, \quad z = r\sin\theta. \tag{1}$$

The relation between the two coordinate systems for a rotating right-handed rotor is

$$x_0 = x, \quad r_0 = r, \quad \theta_0 = \theta - \Omega t, \tag{2}$$

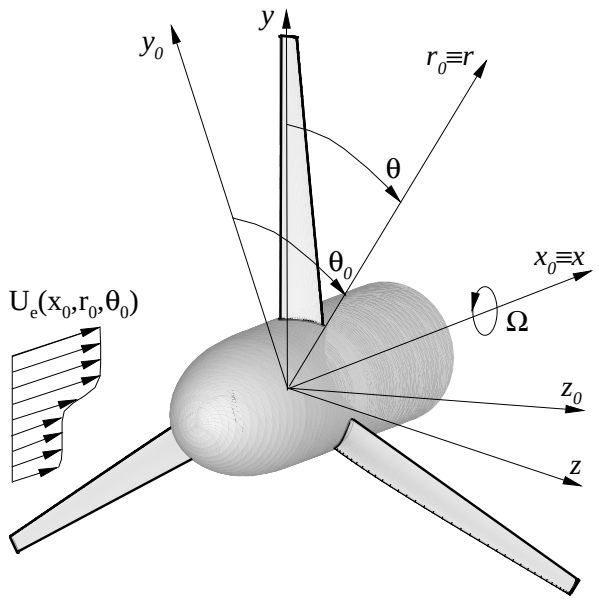

Figure 1: Rotor inflow and coordinate systems.

where $\Omega = |\vec{\Omega}|$ and t is the time. At $t = 0$ the key blade reference line coincides with the y_0 axis.

We will assume that the turbine rotor is subjected to a non-uniform inflow . This inflow is assumed to be steady in the Cartesian inertial frame (x_0, y_0, z_0) and we denote the inflow velocity to the turbine by $\vec{U}_e(x_0, y_0, z_0)$. In the reference frame rotating with the turbine, the undisturbed inflow velocity is time dependent and is given by

$$\vec{V}_\infty(x, r, \theta, t) = \vec{U}_e(x, r, \theta - \Omega t) - \vec{\Omega} \times \vec{x}, \qquad (3)$$

where $\vec{x} = (x, y, z)$.

The fluid flow is assumed to be inviscid and incompressible in an infinite exterior domain to the turbine blades and hub. The perturbation velocity $\vec{v}(x, y, z, t)$ to the inflow is assumed to be irrotational so that it may be written as the gradient of a scalar perturbation potential,

$$\vec{v}(x, y, z, t) = \nabla\phi(x, y, z, t). \qquad (4)$$

In the reference frame rotating with the turbine the flow velocity is

$$\vec{V}(x, y, z, t) = \vec{V}_\infty(x, y, z, t) + \nabla\phi(x, y, z, t). \qquad (5)$$

The perturbation potential satisfies the Laplace equation

$$\nabla^2\phi(x, y, z, t) = 0. \qquad (6)$$

The boundary of the domain consists of the turbine blade surfaces $\mathcal{S}_\mathcal{B}$ and the hub surface $\mathcal{S}_\mathcal{H}$. The perturbation potential must satisfy the following boundary conditions:

$$\nabla\phi \to 0, \quad \text{if} \quad r \to \infty \quad \text{and} \quad x \neq +\infty \qquad (7)$$

at infinity, and a Neumann boundary condition

$$\frac{\partial\phi}{\partial n} \equiv \vec{n} \cdot \nabla\phi = -\vec{n} \cdot \vec{V}_\infty \quad \text{on} \quad \mathcal{S}_\mathcal{B} \quad \text{and} \quad \mathcal{S}_\mathcal{H}, \qquad (8)$$

where $\partial/\partial n$ denotes differentiation along the normal and $\vec{n}$ is the unit vector normal to the surface directed outward from the body.

Since we allow for the existence of circulation around the turbine blades, a vortex sheet is shed from the trailing edge of each blade. From continuity and momentum considerations across a surface of velocity discontinuity, (Saffman, 1992), two boundary conditions apply on the vortex sheet $\mathcal{S}_\mathcal{W}$: the normal component of the fluid velocity is continuous and equal to the normal velocity of the sheet

$$\vec{V}_w \cdot \vec{n} = \vec{V}^+ \cdot \vec{n} = \vec{V}^- \cdot \vec{n} \quad \text{on} \quad \mathcal{S}_\mathcal{W}, \qquad (9)$$

and the pressure is continuous across the vortex wake

$$p^+ = p^- \quad \text{on} \quad \mathcal{S}_\mathcal{W}, \qquad (10)$$

where $\vec{V}$ is the fluid velocity, $\vec{V}_w$ the velocity of the vortex sheet surface $\mathcal{S}_\mathcal{W}$, p is the pressure and the indices $+$ and $-$ denote the two sides of the vortex sheet, arbitrarily chosen on the upper side and lower side of the blade at the trailing edge, respectively.

2.2 Wake Model

The first condition, Equation (9), implies that the vortex sheet moves with the fluid. If $S_w(\vec{x}, t) = 0$ represents the equation of the vortex sheet surface $\mathcal{S}_\mathcal{W}$, then

$$\frac{\partial S_w}{\partial t} + \vec{V}^+ \cdot \nabla S_w = \frac{\partial S_w}{\partial t} + \vec{V}^- \cdot \nabla S_w = 0. \qquad (11)$$

Outside of the vortex sheet the Bernoulli equation applies

$$\frac{\partial\phi}{\partial t} + \frac{p}{\rho} + \frac{1}{2}|\vec{V}|^2 = \frac{p_\infty}{\rho} + \frac{1}{2}|\vec{V}_\infty|^2, \qquad (12)$$

where p_∞ is the pressure of the undisturbed inflow and ρ the fluid density. Applying consecutively the Bernoulli equation at a given point on each side of the vortex sheet and subtracting, we obtain

$$\frac{\Delta p}{\rho} = -\frac{\partial(\Delta\phi)}{\partial t} - \frac{1}{2}\left(\left|\vec{V}^+\right|^2 - \left|\vec{V}^-\right|^2\right), \qquad (13)$$

where $\Delta p = p^+ - p^-$ and $\Delta\phi = \phi^+ - \phi^-$ are the pressure and potential jumps across the sheet, respectively. From the boundary condition, Equation (10), the pressure-jump is zero and Equation (13) becomes

$$\frac{\partial(\Delta\phi)}{\partial t} + \vec{V}_m \cdot \Delta\vec{V} = 0, \qquad (14)$$

where $\vec{V}_m = \frac{1}{2}(\vec{V}^+ + \vec{V}^-)$ is the mean velocity and $\nabla_S(\Delta\phi) = \vec{V}^+ - \vec{V}^-$ is the surface gradient of the potential discontinuity, which is equal to the velocity discontinuity on the wake surface. Equation (14) shows that the potential-jump remains constant following a fluid particle moving on the wake with the velocity $\vec{V}_m$.

In the general case, the instantaneous location of the

wake has to be derived from Equation (11) and the dipole strength from Equation (14), which requires following the motion of the vortex sheet $\mathcal{S}_\mathcal{W}$ in the unsteady flow velocity field. Such calculation is rather involved and beyond the scope of this paper. A considerable simplification is achieved if we assume that $\vec{V}_m$ is constant and equal to the undisturbed time averaged axisymmetric inflow. In the cylindrical coordinate system (x, r, θ),

$$\vec{V}_m = \left(\bar{U}_e(r), 0, \Omega r\right), \tag{15}$$

where $\bar{U}_e(r)$ is the zero harmonic of the axial inflow at the given radius, and Equation (14) becomes

$$\frac{\partial\left(\Delta\phi\right)}{\partial t} + \Omega\frac{\partial\left(\Delta\phi\right)}{\partial\theta} = 0. \tag{16}$$

The solution of Equation (16) is of the form, $\Delta\phi\left(r,\theta,t\right) = \Delta\phi\left(r,t^*\right)$ with $t^* = t^*(\theta,t)$ being a characteristic convection time. Considering that at $t = 0$, $\theta = \theta_{TE}$ we obtain,

$$\Delta\phi\left(r,\theta,t\right) = \Delta\phi\left(r, t - \frac{\theta-\theta_{TE}}{\Omega}\right). \tag{17}$$

The initial condition in the wake is

$$\Delta\phi\left(r,\theta,0\right) = \Delta\phi_{TE}\left(r,0\right) = -\Gamma\left(r,0\right), \tag{18}$$

where Γ is the flow circulation for a circuit around the blade intersecting the wake at the blade trailing edge.

The wake geometry compatible with the assumption for the constant mean convection velocity is a helicoidal wake with pitch angle $\beta = \tan^{-1}\left(\bar{U}_e\left(r\right)/\Omega r\right)$. This wake geometry may be empirically modified to account for steady turbine induced velocities. In such case $|\vec{V}_m|$ is no longer constant in Equation (14) and the solution is of the form, Equation (17), if the tangential induced velocities are assumed zero so that the convection velocity along the wake has the tangential component Ωr. As initial condition a steady flow solution obtained with the time-averaged axisymmetric inflow may be given.

In order to specify uniquely the circulation around the blades it is necessary to impose the Kutta condition at the trailing edge. The Kutta condition states that the velocity must remain bounded at a sharp edge

$$|\nabla\phi| < \infty. \tag{19}$$

2.3 Integral Equation

Applying Green's second identity, assuming for the interior region to $\mathcal{S}_\mathcal{B}$ and $\mathcal{S}_\mathcal{H}$, $\bar{\phi} = 0$, we obtain the integral representation of the perturbation potential at a point p on the body surface,

$$2\pi\phi\left(p,t\right) - \iint\limits_{\mathcal{S}_\mathcal{B}\cup\mathcal{S}_\mathcal{H}}\left[G\left(p,q\right)\frac{\partial\phi}{\partial n_q} - \phi\left(q,t\right)\frac{\partial G}{\partial n_q}\right]dS = \iint\limits_{\mathcal{S}_\mathcal{W}}\Delta\phi\left(q,t\right)\frac{\partial G}{\partial n_q}dS, \tag{20}$$

where $G(p,q) = -1/R(p,q)$, $R(p,q)$ is the distance between the field point p and the point q on the boundary $\mathcal{S} = \mathcal{S}_\mathcal{B}\cup\mathcal{S}_\mathcal{H}\cup\mathcal{S}_\mathcal{W}$. With $\partial\phi/\partial n_q$ on the surfaces $\mathcal{S}_\mathcal{B}$ and $\mathcal{S}_\mathcal{H}$ known from the Neumann boundary condition on the body surface, Equation (8), the Equation (20) is a Fredholm integral equation of the second kind in the dipole distribution $\mu(q,t) = -\phi(q,t)$ on the surfaces $\mathcal{S}_\mathcal{B}$ and $\mathcal{S}_\mathcal{H}$. The Kutta condition, Equation (19), yields the additional relationship between the dipole strength in the $\Delta\phi(q,t)$ wake and the surface dipole strength at the blade trailing edge.

2.4 Velocity, Pressure and Forces

From the potential flow solution on the surface the covariant surface velocity components are calculated by means of a second-order differentiation scheme of the potential relative to the arc lengths on the body surface grid. The pressure on the surface is obtained from the Bernoulli equation, Equation (12). We introduce the pressure coefficient

$$C_p = \frac{p - p_\infty}{1/2\rho V_{ref}^2}. \tag{21}$$

where V_{ref} is a reference velocity. Using Equation (12), the pressure coefficient can be written in terms of the total velocity V_t as

$$C_p = \left(\frac{V_\infty}{V_{ref}}\right)^2 - \left(\frac{V_t}{V_{ref}}\right)^2 - \frac{2}{V_{ref}^2}\frac{\partial\phi}{\partial t}. \tag{22}$$

with $V_\infty = |\vec{V}_\infty|$.

The axial force T and the torque Q on the rotor are obtained by integration of the pressure distribution on the blade surfaces. For the turbine rotor, the non-dimensional quantities used to express the general performance characteristics are the tip-speed-ratio TSR, the axial force coefficient C_T and the power coefficient C_P:

$$TSR = \frac{\Omega R}{U};\;\; C_T = \frac{T}{1/2\rho U^2\pi R^2};\;\; C_P = \frac{\Omega Q}{1/2\rho U^3\pi R^2}, \tag{23}$$

where U is the fluid stream velocity.

3 NUMERICAL METHOD

3.1 Surface Discretisation

For the numerical solution of the integral equation (20) we discretise the blade surfaces $\mathcal{S}_\mathcal{B}$, the hub surface $\mathcal{S}_\mathcal{H}$ and the blade wake surface $\mathcal{S}_\mathcal{W}$ with bi-linear quadrilateral elements which are defined by four points on the body surface. The turbine blade surface is discretised in the spanwise radial direction by a number of strips, extending chordwise from the blade leading edge to the trailing edge. Cosine spacing in the radial and chordwise directions is used. For the discretisation of the hub surface an elliptical grid generator is used, (Sorensen, 1986). The blade wake surface is discretised in the spanwise direction extending downstream from the trailing edge the corresponding strips on the turbine blade.

3.2 Solution of the Integral Equation

The numerical solution of the integral equation (20) is obtained in the time domain at the time steps $n = t/\Delta t$, where δt is the constant time step. The integral equation (20) is solved in space by the collocation method with the element centre point as collocation point. On the blade and hub surfaces, $\mathcal{S}_\mathcal{B}$ and $\mathcal{S}_\mathcal{H}$, the dipole and source distributions are assumed to be constant on each panel. On the wake surface $\mathcal{S}_\mathcal{W}$ piecewise linear or constant dipole distributions are assumed, depending on the specific location of the panel.

Let $\mu_j^k(n) = -\phi_j^k(n)$ be the values at time step n of the dipole strength of the panel S_j^k on the surface of the k^{th} blade-hub sector, $k = 1, \ldots, K$, $j = 1, \ldots, N$, and N being the number of panels of each blade-hub sector; let $\mu_{ml}^k(n) = -\Delta\phi_{ml}^k(n)$ be the values at time step n of the dipole strengths of the boundary between the panel $S_{m,l-1}^k$ and the panel S_{ml}^k of the k^{th} wake, $m = 1, \ldots, N_{Rw}$, $l = 1, \ldots, N_W$, N_{Rw} being the number of panels along the spanwise direction and N_W the number of panels along the streamwise direction of the wake; let $\sigma_j^k(n)$ be the source strength of the panel S_j^k on the surface of the k^{th} blade-hub sector. If, at each time step n, the Equation (20) is exactly satisfied at the central points P_i, $i = 1, \ldots, N_P$ of the $N_P = N \times K$ panels on the surface of the K blade-hub sectors, we obtain a system of algebraic equations in the form

$$\sum_{k=1}^{K}\sum_{j=1}^{N}(\delta_{ij} - D_{ij}^k)\phi_j^k(n) - \sum_{k=1}^{K}\sum_{m=1}^{N_{Rw}}\sum_{l=1}^{N_W} W_{iml}^k \Delta\phi_{ml}^k(n) = -\sum_{k=1}^{K}\sum_{j=1}^{N} S_{ij}^K \sigma_j^k(n), \quad i = 1, \ldots, N_P \tag{24}$$

in which δ_{ij} is the Kronecker delta and D_{ij}^k and S_{ij}^k are the influence coefficients given by

$$\begin{aligned} D_{ij}^k &= \frac{1}{2\pi}\iint_{S_j^k} \frac{\partial}{\partial n_q}\left(\frac{1}{R(p_i,q)}\right) dS \\ S_{ij}^k &= \frac{1}{2\pi}\iint_{S_j^k} \frac{1}{R(p_i,q)} dS \end{aligned}, \tag{25}$$

and W_{iml}^k is a wake influence coefficient which may be written as a linear combination of elementary integrals of the dipole type. The influence coefficients are determined analytically using the formulations of Morino and Kuo (1974). The source strength $\sigma_j^k(n)$ is determined from the boundary condition (8) as

$$\sigma_j^k(n) = -\vec{n}_j^k \cdot \vec{V}_\infty(r_j^k, \theta_j^k, n\Delta t), \tag{26}$$

where $\vec{n}_j^k$ is the unit vector at the control point $(x_j^k, r_j^k, \theta_j^k)$ of the k^{th} blade. To reduce the dimension of the system of equations the boundary condition is only applied at the key blade $k = 1$. Hence, the contributions of the other blades $(k > 1)$ are assumed to be known when solving for the key blade. Furthermore, only the first strip of dipoles in the wake close to the trailing edge of the key blade is treated as being part of the unknowns.

The solution in the rotating frame, i.e. on the key blade, is periodic in time with a period, in general, equal to the time of a turbine revolution. The non-dimensional time step $\Delta\theta = \Omega\Delta t$ is introduced. We denote the total number of time steps by $N_t = N_{rev} \times N_\theta$, where N_{rev} is the number of revolutions (or periods) for the time integration and $N_\theta = 2\pi/\Delta\theta$.

3.3 Numerical Kutta Condition

The value of the dipole strength at the blade trailing edge $\Delta\phi$ is determined by the application of a Kutta condition. The Morino Kutta condition equates the dipole strength at the trailing edge to the potential-jump between the two sides of the blade

$$\Delta\phi = \phi^+ - \phi^- \tag{27}$$

in which ϕ^+ and ϕ^- denote the values of the potentials at the first and last collocation points of the m^{th} blade strip. Alternatively, a non-linear pressure Kutta condition may be applied, requiring that the pressure is equal on both sides of the blade trailing edge. In the present work, due to the non-linear character of the pressure, the dipole strength at the blade trailing edge is obtained by the method of Newton-Raphson.

4 VISCOUS EFFECTS ON BLADE FORCES

In this section we consider quasi-steady corrections due to viscous effects to the ideal turbine axial force and power calculated with the panel method. The viscous forces on the turbine blades are calculated using the concept of section lift and drag force that can be derived from two-dimensional lift and drag data.

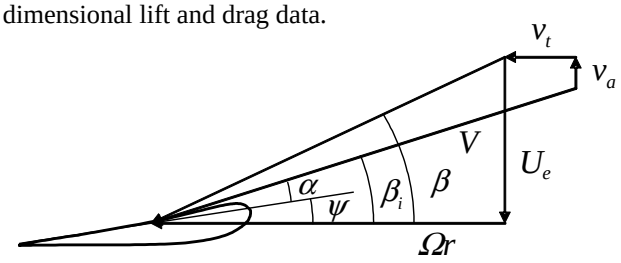

Figure 2: Velocity triangle on a blade section.

Let us consider the velocity triangle at a turbine blade section of radius r as shown in Figure 2. The inviscid lift force L_i is, per definition, perpendicular to the incoming velocity V to the blade section. The hydrodynamic pitch angle β_i can be determined from the elementary contributions to the ideal axial force dT_i and torque dQ_i by the relation

$$\tan\beta_i = \frac{dQ_i}{r dT_i}. \tag{28}$$

The section angle of attack is related to the hydrodynamic pitch angle by

$$\alpha = \beta_i - \psi, \tag{29}$$

where ψ is the section pitch angle. With viscous effects, the elementary contributions to the axial force and torque are

$$\begin{aligned} dT_v &= (L_v \cos\beta_i + D \sin\beta_i) dr \\ dQ_v &= (L_v \sin\beta_i - D \cos\beta_i) r dr \end{aligned}. \tag{30}$$

The viscous lift force L_v (per unit length) of the section is given by

$$L_v = L_i \frac{C_{L_v}}{C_{L_i}}, \tag{31}$$

where C_{L_v} and C_{L_i} are the section viscous and inviscid lift coefficients of the blade section at the angle of attack α, respectively. The drag force (per unit length) is

$$D = C_D \frac{1}{2} \rho V^2 c, \tag{32}$$

where C_D is the section drag coefficient at the angle of attack α, Equation (29), and c the section chord. The incoming velocity V can be calculated by the Kutta-Joukowski law in steady flow:

$$L_i = \rho V \Gamma. \tag{33}$$

If viscous corrections on the lift force are ignored C_{L_v}/C_{L_i} is equal to 1 in Equation (31). The total axial force and torque are obtained by integration of the elementary contributions along the radial spanwise direction.

5 RESULTS

5.1 General

The turbine rotor described in Bahaj et al. (2007b) is considered. For this rotor a considerable set of experimental data obtained from cavitation tunnel and towing tank tests is available in the literature, (Bahaj et al., 2007b). The turbine is a three-bladed turbine with NACA 63-8XX sections. The standard geometry has a pitch angle at the blade root equal to 15 degrees, corresponding to 0 degrees pitch setting at the tip. In the present work, 5 and 10 degrees pitch setting angles have been considered. The detailed geometry of the marine current turbine is given in Bahaj et al. (2007b).

Figure 3 shows a typical panel arrangement of the turbine rotor with the set angle of 5 degrees as well as the prescribed wake. Each turbine blade is discretised with 60 and 31 panels in the chordwise and radial directions, respectively. The blade wake is discretised with 180 panels along the streamwise direction and 30 panels along the radial direction, which corresponds to an axial length of 3 turbine radii. The pitch of the helicoidal lines is constant and was obtained from the lifting line theory with optimum circulation distribution, (Falcão de Campos, 2007), for a

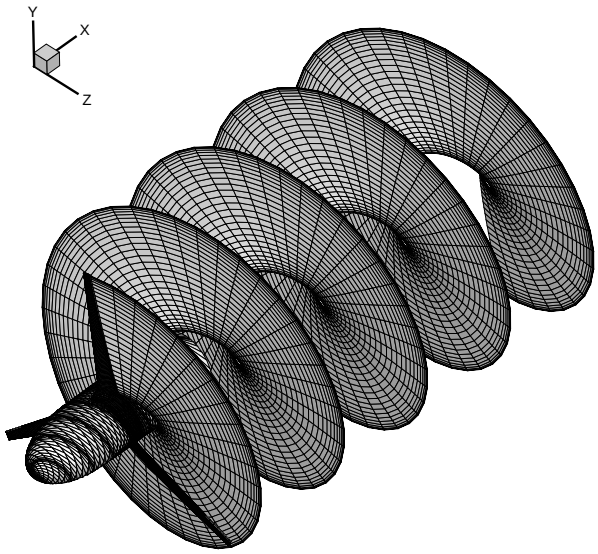

Figure 3: Panel arrangement with wake grid. Note that only one wake surface is shown.

$TSR = 6$. The hub is discretised with 80 panels along the axial direction and 36 panels along the circumferential direction.

Calculations have been performed with the panel code PROPAN for straight and yawed inflow conditions in a wide range of tip-speed-ratios. The calculations presented refer to the blade grid 60×31 (Figure 3). This discretisation provides a reasonably converged potential flow solution, (Baltazar and Falcão de Campos, 2008). The system of equations was solved with a direct method (LU factorisation). An iterative pressure Kutta condition to a precision of $|\Delta C_p| \leq 10^{-3}$ at the blade trailing edge was used. The yawed inflow is defined by

$$\begin{aligned} &\vec{U}_e(x, r, \theta - \Omega t) = \\ &U \left[\cos\gamma, \sin\gamma \sin(\theta - \Omega t), \sin\gamma \cos(\theta - \Omega t)\right] \end{aligned} \tag{34}$$

where γ is the yaw angle with the turbine rotation axis. For the calculations, $N_\theta = 40$ time steps per revolution are considered, which leads to an angular step of 9 degrees. For the number of revolutions $N_{rev} = 5$ is used.

5.2 Comparison With Experimental Data

The comparison between the axial force and power coefficients at straight inflow conditions predicted with the present panel method and an analysis code based on the lifting line theory (Falcão de Campos, 2007), with the experimental data (Bahaj et al., 2007b) is shown in Figures 4 and 5, for the turbine rotor with set angles of 5 degrees and 10 degrees, respectively. The numerical calculations are presented for a helicoidal vortex wake with pitch distribution determined from the lifting line theory with optimum circulation distribution, (Falcão de Campos, 2007). The effect of the vortex wake pitch has been investigated in steady flow in Baltazar and Falcão de Campos (2008). A

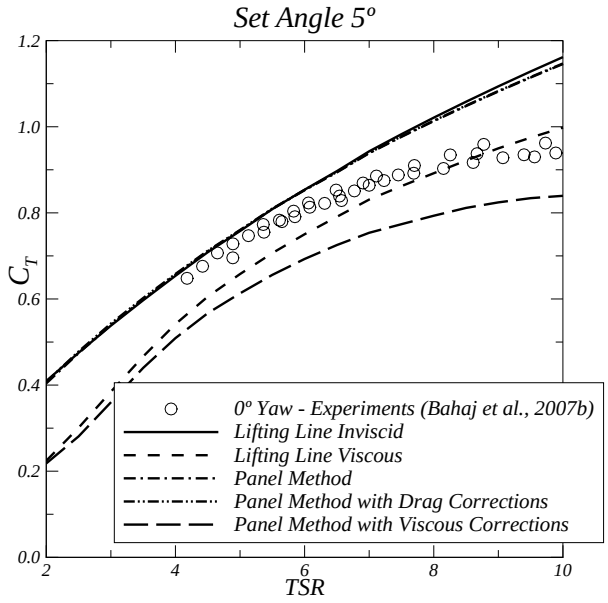

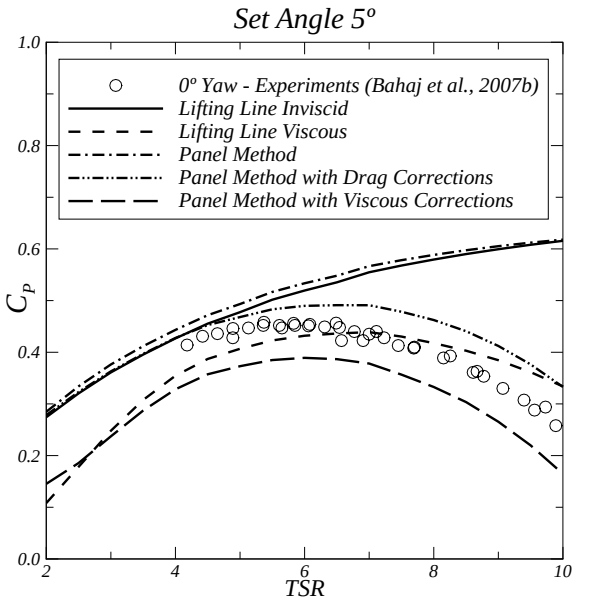

Figure 4: Comparison with experimental data at 0° yaw angle for 5° set angle. C_T (top) and C_P (bottom).

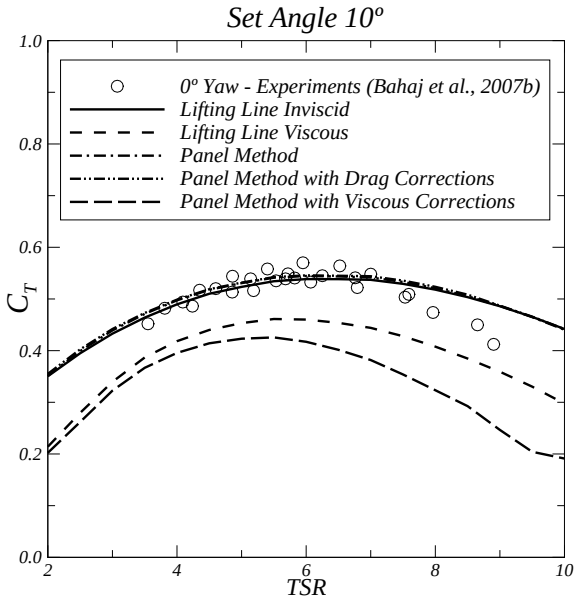

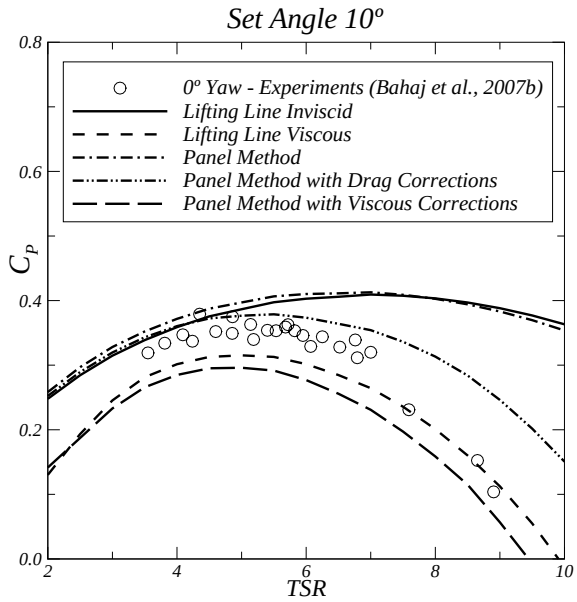

Figure 5: Comparison with experimental data at 0° yaw angle for 10° set angle. C_T (top) and C_P (bottom).

strong influence of the pitch of the vortex lines was found in the performance predictions of the turbine rotor with the panel method. The difference between the present choice and the use of a transition wake starting from the geometric pitch is minor.

The panel method and lifting line calculations were carried out without and with viscous effects. Corrections in the inviscid lift force and the contribution of section drag force were taken into account. For illustrate the two effects the influence of only the section drag in the axial force and power coefficients was also considered. For the two-dimensional section data, the inviscid lift curve of blade sections has been derived from 2D panel code computations (Vaz, 2005), and the drag was set to zero. The viscous lift and drag coefficients of the blade sections have been taken from the XFoil computations published in Bahaj et al. (2007a).

Similar results are obtained between the present method and the lifting line theory in the inviscid mode. For this case, a reasonable agreement with the experimental data in the range of TSR between 4 and 6 for both blade pitch settings is seen in the axial force coefficient. We note that $TSR = 6$ is reported as the design condition for the pitch set angle of 5 degrees, (Bahaj et al., 2007b). For the power coefficient the calculations are somewhat higher than the experimental data in the same range of TSR values. This is to be expected for a fully inviscid calculation near design condition where viscous effects tend to be relatively small. For TSR lower than 4 the inviscid calculation will overpredict the power curve, as increasing separation phenomena

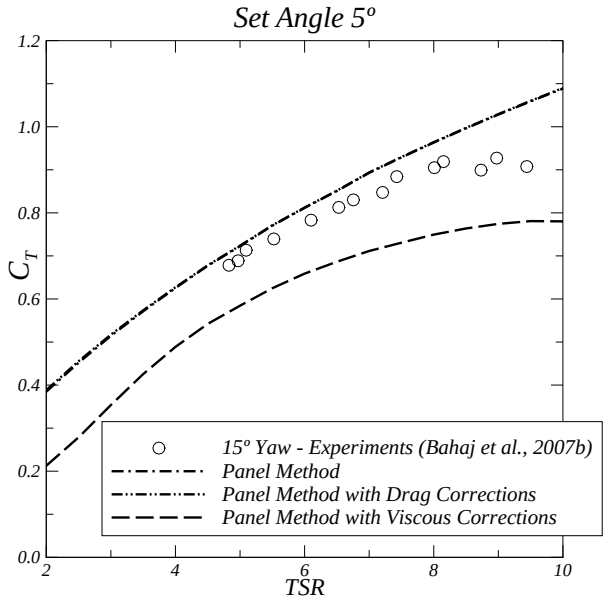

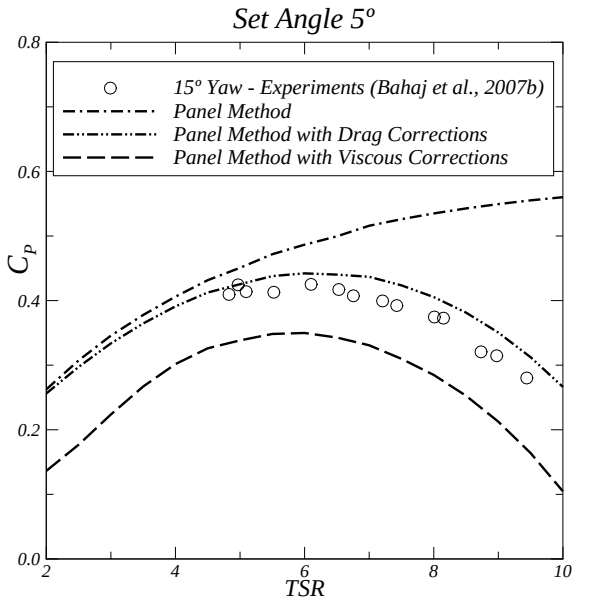

Figure 6: Comparison with experimental data at 15° yaw angle for 5° set angle. C_T (top) and C_P (bottom).

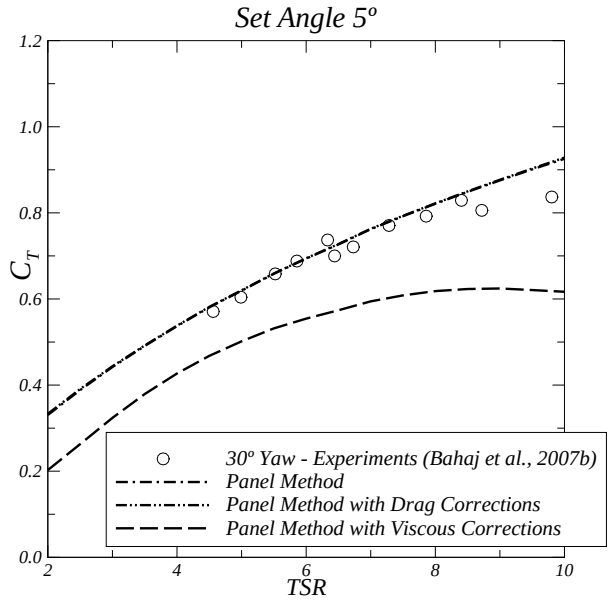

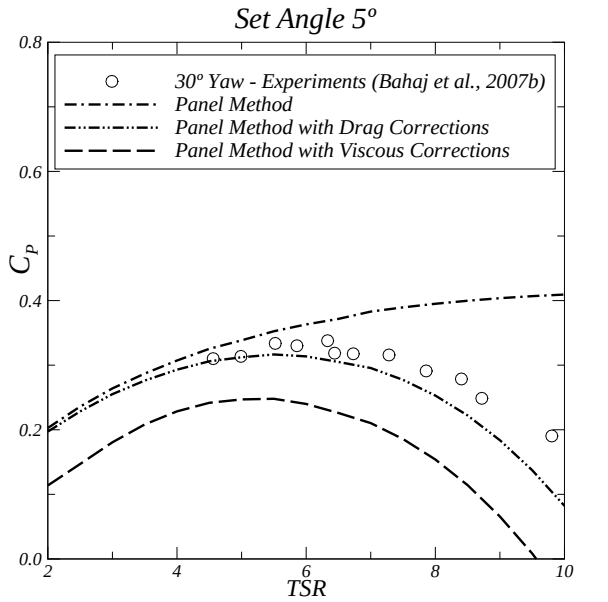

Figure 7: Comparison with experimental data at 30° yaw angle for 5° set angle. C_T (top) and C_P (bottom).

is likely to occur starting from the inner parts of the blades closer to the hub. For TSR values larger than 6 the inviscid calculations are seen to considerably overpredict the axial force and power data.

The inclusion of the viscous effects in both panel method and lifting line calculations is seen to significantly decrease the axial force and power curves. From the comparison with the experiments, a strong reduction of the predicted axial force and power coefficients with viscous corrections is seen in the panel method calculations. However, considering only the drag force in the viscous corrections a smaller decrease in the power coefficient is obtained. This result indicates that the viscous corrections in the lift force may be overestimated in the present panel method calculations. The results obtained with the lifting line theory using viscous effects are in closer agreement with the experimental data.

The calculated mean axial force and power coefficients at different yaw angles for the blade set angles of 5 and 10 degrees are compared with the experimental data, (Bahaj et al., 2007b), in Figures 6 to 8. All cases show a consistent decrease in the mean axial force and power coefficients with increasing yaw angle. A fair to good agreement with experimental data for the inviscid axial force is seen. For the inviscid power coefficient the panel method calculations are higher than the experimental data, especially for TSR values larger than 6. Again, the inclusion of viscous effects strongly decreases the axial force and power coefficients. By including only the drag force a smaller reduction is obtained in the turbine power. In addition, a small effect

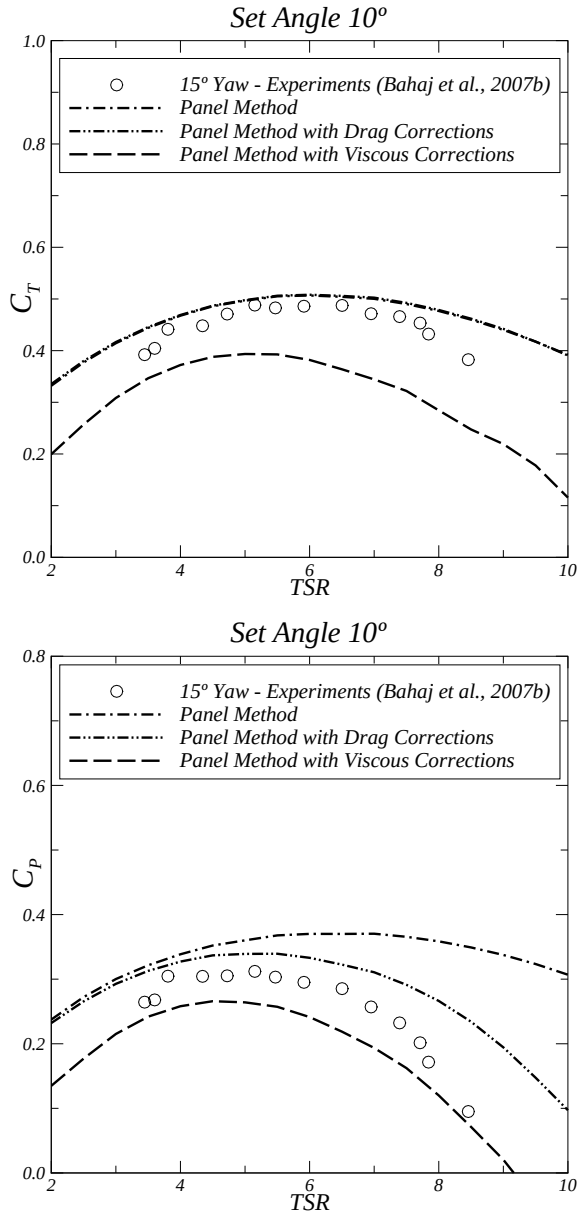

Figure 8: Comparison with experimental data at 15° yaw angle for 10° set angle. C_T (top) and C_P (bottom).

of the drag force in the turbine axial force is obtained for these operating conditions.

6 CONCLUSIONS

Unsteady potential flow calculations with a low order potential based panel method were performed for a horizontal axis marine current turbine. Calculations were made at straight and yawed inflow conditions for two blade pitch settings. A simple empirical wake model is assumed for the turbine wake.

A fair to good agreement with the experimental performance data was found near the design condition where viscous effects are likely to be small. The effect of yaw in the performance coefficients seems to be reasonably captured near design condition. Viscous effects need to be taken into account for the predictions at off-design conditions. The inclusion of the viscous corrections is seen to significantly decrease the axial force and power curves, bringing the calculations to a closer agreement with the experimental data, especially for large tip-speed-ratios.

The authors believe the method may prove to be a valuable tool for the hydrodynamic analysis of marine current turbines. However, a more accurate prediction of the vortex wake seems to be required for the improvement of the present method.

REFERENCES

Bahaj, A., Batten, W., and McCann, G. (2007a). 'Experimental verifications of numerical predictions for the hydrodynamic performance of horizontal axis marine current turbines'. Renewable Energy, 32(15):2479 – 2490.

Bahaj, A., Molland, A., Chaplin, J., and Batten, W. (2007b). 'Power and thrust measurements of marine current turbines under various hydrodynamic flow conditions in a cavitation tunnel and a towing tank'. Renewable Energy, 32(3):407 – 426.

Baltazar, J. (2008). On the Modelling of the Potential Flow About Wings and Marine Propellers Using a Boundary Element Method. PhD Thesis, Instituto Superior Técnico, Technical University of Lisbon.

Baltazar, J. and Falcão de Campos, J. (2006). 'Unsteady potential flow calculations of marine propellers using BEM'. In Conferência Nacional de Métodos Numéricos em Mecânica de Fluidos e Termodinâmica, Monte de Caparica, Portugal.

Baltazar, J. and Falcão de Campos, J. (2008). 'Hydrodynamic analysis of a horizontal axis marine current turbine with a boundary element method'. In Proceedings of the 27th International Conference on Offshore Mechanics and Artic Engineering, OMAE, Estoril, Portugal.

Falcão de Campos, J. (2007). 'Hydrodynamic power optimization of a horizontal axis marine current turbine with lifting line theory'. In Proceedings of the Seventeenth International Offshore and Polar Engineering Conference, ISOPE, volume 1, pages 307 – 313, Lisbon, Portugal.

Kerwin, J., Kinnas, S., Lee, J.-T., and Shih, W.-Z. (1987). 'A surface panel method for the hydrodynamic analysis of ducted propellers'. SNAME Transactions, 95:93 – 122.

Morino, L. and Kuo, C.-C. (1974). 'Subsonic potential aerodynamics for complex configurations: A general theory'. AIAA Journal, 12(2):191 – 197.

Saffman, P. G. (1992). Vortex Dynamics. Cambridge University Press.

Sorensen, R. L. (1986). 'Three-dimensional elliptic grid generation about fighter aircraft for zonal finite-difference computations'. In AIAA-86-0429. AIAA 24th Aerospace Sciences Conference, Reno, NV.

Vaz, G. (2005). Modelling of Sheet Cavitation on Hydrofoils and Marine Propellers Using Boundary Element Methods. PhD Thesis, Instituto Superior Técnico, Technical University of Lisbon.